Int J Thermophys (2008) 29:1987–1996
DOI 10.1007/s10765-008-0513-y

Phonon Contribution to Thermal Boundary Conductance at Metal Interfaces Using Embedded Atom Method Simulations

R. N. Salaway · P. E. Hopkins · P. M. Norris · R. J. Stevens

Published online: 7 October 2008

Abstract The phonon contribution to the thermal boundary conductance (TBC) at metal–metal interfaces is difficult to study experimentally, and it is typically considered negligible. In this study, molecular dynamics simulations (MDS), employing an embedded atom method (EAM) potential, are performed to study the phonon contribution to thermal transport across an Al–Cu interface. The embedded atom method provides a realistic model of atomic behavior in metals, while suppressing the effect on conduction electrons. In this way, measurements on the phonon system may be observed that would otherwise be dominated by the electron contribution in experimental methods. The relative phonon contribution to the TBC is calculated by comparing EAM results to previous experimental results which include both electron and phonon contributions. It is seen from the data that the relative phonon contribution increases with decreasing temperature, possibly accounting for more than half the overall TBC at temperatures below 100 K. These results suggest that neglect of interfacial phonon transport may not be a valid assumption at low temperatures, and may have implications in the future development of TBC models for metal interfaces.

Keywords Embedded atom method · Interface · Metal · Molecular dynamics simulations · Phonon · Thermal boundary conductance

R. N. Salaway · P. E. Hopkins · P. M. Norris (✉)
Microscale Heat Transfer Laboratory, Department of Mechanical and Aerospace Engineering, University of Virginia, Charlottesville, VA 22903, USA
e-mail: pamela@virginia.edu

R. J. Stevens
Department of Mechanical Engineering, Rochester Institute of Technology, Rochester, NY 14623, USA

1 Introduction

With consumer demands for ever smaller and faster electronics, thermal management of these devices has become more difficult with decreasing device size. For example, the thermal management of laptop computers is known to greatly affect the mean time to failure (MTTF) [1]. In these devices, many integrated circuits (ICs) must be cooled by limited airflow constricted by chassis size. Typically, ICs are composed of metal oxide semiconductor (MOS) transistors that employ metal packaging to increase efficiency of thermal throughput to the metal heat sink [2]. This contact between the metal heat sink and metal transistor packaging is the point at which heat is drawn from the transistor and is a point which has great influence on the efficiency of thermal management. Therefore, the heat transfer across these boundaries, known as the thermal boundary conductance (TBC), is of great interest.

When thermal transport occurs across the interface of two different materials, there exists an observable discontinuity in temperature profile at the infinitesimal boundary. This temperature drop is the result of a resistance to thermal transport across material interfaces, known as the thermal boundary resistance or Kapitza resistance [3]. The inverse of the Kapitza resistance is the TBC, denoted as h_{BD}, and can relate the heat flux across an interface, $\dot{q}$, to the temperature drop, ΔT, by the following equation:

$$\dot{q} = h_{\mathrm{BD}} \Delta T \tag{1}$$

The TBC is a parameter of interest, as it defines the thermal throughput at any contact point. Previously neglected in large-scale device analysis, the TBC becomes increasingly important as device size continues to decrease [4]. With growing interest in nanotechnology, the TBC will play a major role in design optimization as these devices become increasingly defined by their boundaries. For example, semiconductor superlattices are found to have thermal properties much different than the bulk properties of their components, due to the many multilayer interfaces [5]. For these reasons, a thorough understanding of the fundamental processes occurring at thermal boundaries is essential for designing nanoscale devices [6].

Thermal transport in metals occurs by means of two energy carriers: phonons and free electrons. As the free electron concentration typically outnumbers the phonon concentration by several orders of magnitude, the contribution from phonons is considered insignificant and often neglected from thermal models of metals [7]. Furthermore, the dominating presence of free electrons means experimental methods typically measure the electron contribution while any contribution from the phonon system is obscured in the measurement. As a result of all these factors, little is quantitatively known about the phonon contribution to thermal processes in metal systems. Just as the TBC has only recently become an increasingly important consideration with the advent of nanoscale devices, so too is the time approaching when our knowledge of the TBC is exact enough to warrant consideration of all energy carriers.

Several well-established continuum models predict the TBC between solids. A commonality between the models is the assumption that phonons are wholly responsible for all thermal transport across an interface. While this may be a valid assumption when considering interfaces between dielectrics, these continuum models are unable to predict the TBC at metal–metal interfaces, due to the overwhelming presence of

conduction electrons and their contribution to interfacial transport. Perhaps one of the most widely used continuum models is the diffuse mismatch model (DMM) developed by Swartz and Pohl [8,9]. This model assumes each incident phonon is diffusely scattered at the interface, thereby losing all memory from where it came. The probability of transmission simply depends on the relation of the density of states of the two materials and, therefore, the probability of the phonon existing in one material versus the probability of existing in the other [10]. The DMM has been shown to yield reasonable results for some systems [4] when compared to experimental measurements on dielectric interfaces well below the Debye temperature [8,9]. Limitations of the DMM have been observed [11] in that the model is less accurate at elevated temperatures (typically above 100 K), and it cannot accurately predict the TBC at metal–metal interfaces due to the neglect of the electron contribution.

2 Simulation

2.1 Atomic Potential

Molecular dynamics simulations (MDS) are implemented to study the phonon contribution to the TBC at the atomic level. An advantage of MDS is the necessary assumptions are far fewer than those required in a continuum model. All that is required is to define an atomic lattice structure and an inter-atomic potential. The embedded atom method (EAM) is an inter-atomic potential that has been shown to realistically describe metal systems [12]. It is termed a many-body potential, because it not only accounts for pair-wise potentials between individual atoms, but also incorporates an environmental term which describes the many-body effects from the surrounding neighbors. This environmental term makes the potential suitable in describing metals, where many-body interactions are important [13];

$$U_i = \frac{1}{2}\sum_{j\neq i} \Phi_i\left(r_{ij}\right) + D_i\left(\rho_i\right) \tag{2}$$

The embedded atom method is aptly named, as it yields the potential energy, U_i, necessary to embed atom i from free space into the local environment described by the surrounding neighbors. Equation 2 shows that this potential is a function of the pair-wise potential term, Φ_i, and the environmental term, $D_i\left(\rho_i\right)$. The pair-wise term is evaluated over all nearest neighbors within a cutoff distance, and is a function of r_{ij}, the distance between the atom of consideration and each neighboring atom. The environmental term is a function of ρ_i, the local electronic density into which atom i is being embedded:

$$\rho_i\left(r_{ij}\right) = \sum_{j\neq i} f_j\left(r_{ij}\right) \tag{3}$$

where f_j is the contribution to this local electronic density from each neighboring atom j. The EAM has been derived in previous literature along with empirical determination of parameters used to describe real systems [13,14].

It is important to note that the EAM only accounts for the presence of electrons by considering the contribution of bound electrons to atomic potentials. Nowhere is the presence of free conduction electrons considered. While the EAM can adequately model the atomic interactions of metal systems, its description of processes involving conduction electrons, such as thermal transport, will be limited to pure consideration of the phonon system. In this way, the EAM allows for something unattainable in experiments. By neglecting the presence of conduction electrons, the EAM is able to examine the phonon contribution to the TBC, something that cannot be isolated from the dominating electron contribution by experimental methods. Since the electron contribution to atomic interactions is accounted for via the environmental term, the lattice system, and consequently the phonon system, behaves as it would in the presence of conduction electrons.

2.2 Computational Cell

The computational cell was set up to simulate thermal conduction across the interface of two metal films by nonequilibrium molecular dynamics (NEMD). Parameters were chosen to model a thin Al film adjoining a thin Cu film. The computational cell comprised two separate lattice and atomic types, separated by an interface in the $x-y$ plane. Side A is an FCC lattice with a lattice constant of 4.05 Å and an atomic mass of 26.98 a.m.u, representing the Al film [7]. Side B is also an FCC lattice with a lattice constant of 3.60 Å and atomic mass of 63.60 a.m.u, representing the Cu film [7]. The dimensions of side A are $16 \times 16 \times 15$ unit cells in the x-, y-, and z-directions, respectively, and those of side B are $18 \times 18 \times 15$ unit cells. Both sides have two atomic planes per unit cell, thus creating a computational cell of 30 Al atomic planes in the z-direction adjoining 30 Cu atomic planes in the z-direction, separated by an interface in the x–y plane.

Having defined the computational cell, an interface between two thin films is simulated through the use of boundary conditions. Periodic boundary conditions are employed in the x- and y-directions, while free boundary conditions are employed in the z-direction. In this way, the computational cell is projected out in the x- and y-directions, creating an interface between two films of infinite cross-sectional area and each having a finite thickness of 30 atomic planes in the z-direction. The equations of motion for all atoms in the system were integrated using the Nordsieck fifth-order predictor–corrector algorithm. A reasonable time step of integration was found to be 5 fs. The use of smaller time steps in preliminary trial simulations did not significantly affect simulation results.

The temperature of a system of particles can be related to their individual velocities. If the system of particles is taken to be all the atoms in one atomic plane, then an atomic plane temperature can be defined [15] as

$$T_{\text{plane}} = \sum_{i=1}^{N_{\text{plane}}} \frac{m_i {v_i}^2}{3k_{\text{B}} N_{\text{plane}}} \tag{4}$$

Equation 4 shows how the planar temperature can be calculated as a function of each atom's mass (m_i), velocity (v_i), and the Boltzmann constant, k_{B}, when evaluated over

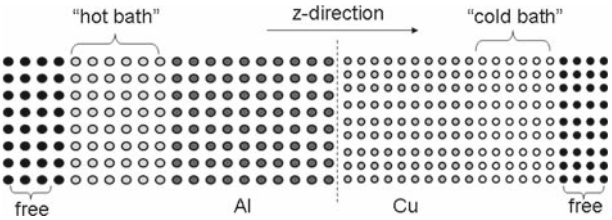

Fig. 1 Schematic of the computational cell. Thermal energy is added to the hot bath and removed from the cold bath to induce a steady-state heat flux across the interface in the positive z-direction

all N_{plane} atoms in the plane. Two regions are defined as "hot bath" and "cold bath" regions. These are pre-designated regions consisting of six atomic planes into which thermal energy can either be added or subtracted by a linear scaling of the atomic velocities. Figure 1 shows a schematic of the computational cell. Note that the number of central atomic planes has been reduced for clarity in the presentation. When orientated with the increasing z-direction to the right, the Al section is to the left of the Cu section. The first four atomic planes on either side have free boundary conditions, and are not included in any calculations. They are only meant to provide a more realistic boundary for the inner atoms. The next five atomic planes to the right of the free boundary planes in the Al film make up the "hot bath" region. Here, thermal energy is added to the Al film through a linear increase in atomic velocities. Likewise, the first five atomic planes to the left of the free boundary planes in the Cu film make up the "cold bath" region, where energy is taken from the system through a scaling down of atomic velocities.

2.3 Procedure

With the computational cell defined, a steady-state temperature profile can be created through the repeated manipulations of the hot and cold bath regions. A desired temperature is chosen for each of the two regions. Initially, the computational cell is heated to the average of the two desired temperatures. Once the overall temperature has become stable, the temperatures in the hot and cold bath regions are monitored after a repeated interval of computational iterations. If the measured temperature in any of the bath-region atomic planes differs from the pre-designated desired temperature, thermal energy is adjusted through scaling of atomic velocities.

After several tens of thousands of iterations, the temperatures in the bath regions become stable, and the energy added to the hot bath is essentially equal to the energy removed from the cold bath. In this way, a steady-state temperature profile is created with a constant heat flux crossing the interface. The heat flux is calculated when the energy added or subtracted from the bath regions is divided by the cross-sectional area of the computational cell and the time interval over which it was added or subtracted. The temperature profile can be determined by Eq. 4 for each atomic plane. A more stable profile is obtained when each atomic plane temperature is averaged over many time steps. In this way, a time-averaged temperature profile is generated which eventually stabilizes into a constant configuration.

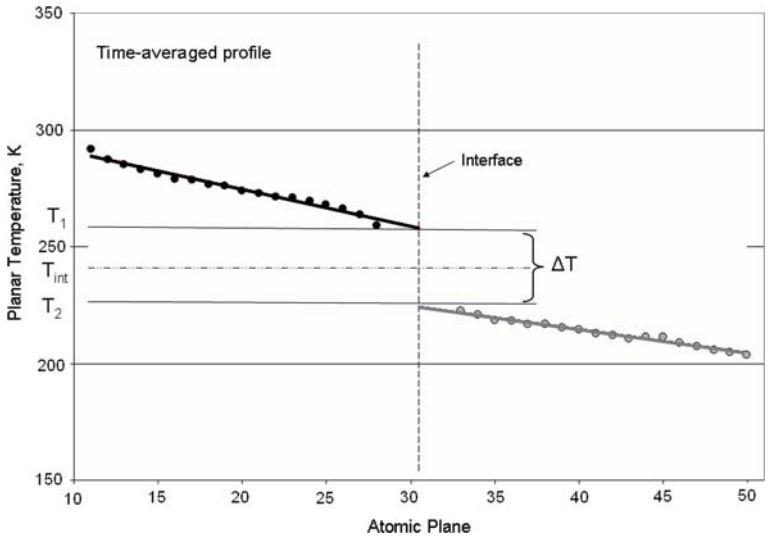

Fig. 2 A linear fit is applied to the central atomic planes. The planes closest to the interface and those contained in the bath region are neglected for accuracy

Once the time-averaged temperature profile becomes stable, and further iterations do not significantly alter the calculations, a linear fit is applied to the 18 central atomic planes on each side of the interface. Planes in the bath regions and the two atomic planes immediately adjacent to the interface on either side are discarded for accuracy, and a linear fit is applied to atomic planes 11 through 28 on the Al side and planes 33 through 50 on the Cu side. Figure 2 is an example of a time-averaged temperature profile after a linear fit. The linear fit of both sides is projected to the interface, and the difference in the two points of intersection is taken to be the temperature drop at the interface. Having determined both the steady-state heat flux and the temperature drop at the interface, the thermal boundary conductance can be calculated from Eq. 1.

The thermal boundary conductance over a given time *interval* is defined as the average flux divided by the average temperature drop over that interval. Once a steady state has been reached, the measuring and averaging of the thermal boundary conductance over some time interval is begun. A typical time interval over which the TBC is averaged is 200 time steps or 1 ps. Then those interval values are continually averaged with subsequent interval measurements. It is seen that when initial measurements of the average thermal boundary conductance are taken, the values can be noisy, but tend to settle down to a reasonably stable value after several tens of thousands of measurements. This process is repeatable and by observing the fluctuation in averages, a projected end value can be predicted, and it can be seen when the final calculations are reasonably stable and consistent with that value. When additional time steps and average measurements produce no significant variations in the overall average value, the final measurement of the thermal boundary conductance for that simulation is recorded.

This process used to obtain a measurement of the TBC can be repeated to investigate the uncertainty of measurement. While simulations of different initial configuration

(i.e., simulations to yield different boundary temperatures) resulted in different confidence intervals, the overall average 95 % confidence interval for all simulations was found to be $\pm 2.4 \times 10^6\ \mathrm{W \cdot m^{-2} \cdot K^{-1}}$.

The temperature of the interface is taken to be the midpoint of the two interception points. Adjusting the choice in bath-region temperatures will result in different values of interfacial temperature. The TBC was systematically observed over a range of final interfacial temperatures. Also affected by the choice in bath-region temperatures are the steady-state heat flux and temperature drop at the interface. As the TBC is defined as the ratio of heat flux to temperature drop at the interface, a higher temperature drop should, in theory, force a higher steady-state heat flux and result in the same final TBC at the interface for a given interfacial temperature, independent of the temperature drop. Preliminary trial simulations were consistent with theory and have shown that the temperature drop does not significantly affect the final result. It was observed, however, that simulations involving higher temperature drops, or larger discrepancies in bath-region temperatures, reached equilibrium faster than those including smaller temperature drops. Thus, prescribed bath-region temperatures were chosen to systematically provide a range of final interfacial temperatures, while maintaining computational efficiency. Although it was not possible to prescribe the final interfacial temperature by the initial configuration choices, a sufficient range of bath-region temperatures provided a sufficient range in resultant interfacial temperatures.

3 Results

3.1 Comparison

As mentioned earlier, the DMM is a widely used continuum model and assumes phonons are wholly responsible for interfacial thermal transport. The DMM thus would not yield results consistent with experiment, when applied to an Al–Cu interface where free electrons are the dominant means of thermal transport. However, both the current simulation and the DMM can be used to predict the phonon contribution to the TBC in an Al–Cu interface. Figure 3 shows a comparison between the simulation results and the DMM predictions for the TBC in an Al–Cu interface over a range of temperatures. The simulation results exhibit the same general trend shown in the DMM, and are reasonably comparable in value.

Though widely used, the DMM can be found to produce predictions of limited accuracy. Notably, it has been found that the DMM may tend to under-predict the TBC at very low temperatures (<100 K) while over-predicting the TBC at higher temperatures when employing a Debye density of states [11], as is the case in Fig. 3. This flaw in the DMM is consistent with the discrepancy between the DMM and simulation results.

3.2 Phonon Contribution

Any experimental measurements of the TBC at a metal–metal interface will include the overwhelming contribution from electrons. Gundrum et al. [16] performed

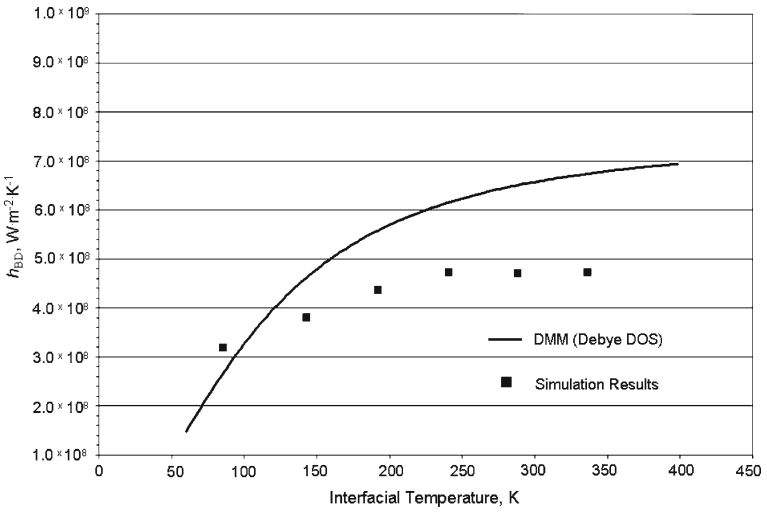

Fig. 3 Simulation results for the TBC compared to the DMM employing the Debye density of states

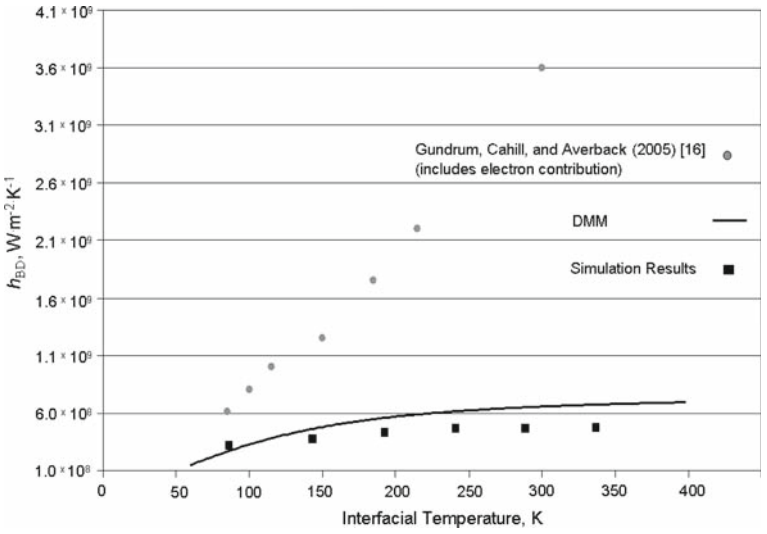

Fig. 4 Simulation and DMM predictions of the TBC compared to the experimental measurements of Gundrum et al. [16] for an Al–Cu interface. The drastic under-prediction is expected as both model and simulation neglect the contribution from free electrons

measurements of the TBC on an Al–Cu interface over the same temperature range studied in this paper. Their results are shown in Fig. 4, compared to the DMM and the simulation results. As expected, the experimental measurements of Gundrum et al. are far greater than predicted by the simulation which only models the phonon contribution to the TBC.

As mentioned above, the simulation provides a way of intentionally suppressing the electron contribution in order to study the relative effects of phonon thermal transport

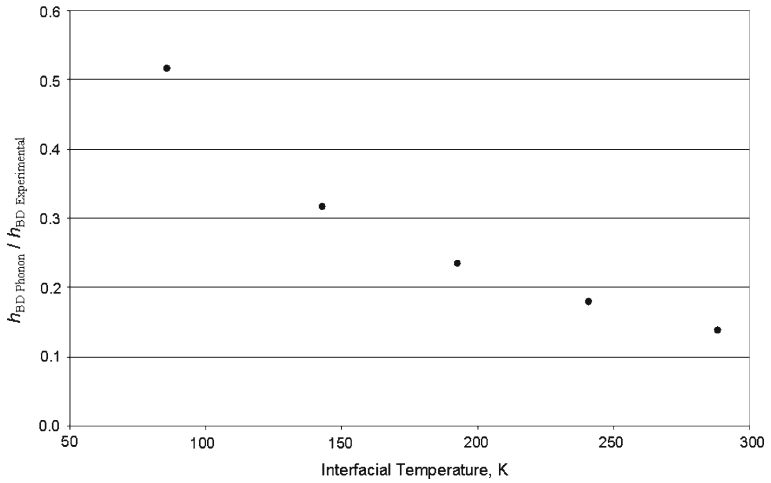

Fig. 5 Relative phonon contribution to the overall TBC as a function of interfacial temperature. The ratio is calculated by dividing simulation results by experimental measurements of Gundrum et al. [16]

at interfaces that are dominated by electron conduction, which is typically considered to be negligible [16]. A relative phonon contribution to the overall TBC can be defined by dividing the simulation results by the experimental measurements of Gundrum et al. While the experimental results are measurements of the overall TBC in an Al–Cu interface, the simulation results are a measure of the phonon contribution to the overall thermal transport. Thus, the ratio of the two measurements can be thought of as a measure of the relative contribution from the phonon system to the overall TBC. In Fig. 5, this ratio is plotted over a range of temperatures. From the data, it is seen that while the contribution from the phonon system is approaching 10 % at room temperature, there seems to be an increase in the phonon contribution with decreasing temperature. Notably, at temperatures below 100 K, the phonon system appears to be responsible for more than half the overall interfacial thermal transport.

4 Conclusions

Molecular dynamics simulations are employed to examine the contribution to the TBC from the phonon system at an Al–Cu interface over a range of temperatures. These methods allow for the systematic study of the phonons in systems where experimental measurements would be overwhelmingly dominated by electrons. From the data, it appears that the phonon contribution to the TBC tends to increase with decreasing interfacial temperature. While the phonon system only contributes roughly 10 % to the overall TBC at temperatures around 300 K, it seems the relative importance of the phonon contribution may actually increase with decreasing temperature. While further investigation is still suggested, as consideration of quantum effects may prove necessary, this study shows a discernable trend. Currently, there exists no widely accepted and proven model for the TBC at metal interfaces. Attempts to develop a model have

neglected the phonon contribution [16]. Future models of the TBC at metal interfaces may need to reconsider the contribution from the phonon system when modeling at low temperatures.

Acknowledgments This work was funded through the National Science Foundation (CTS—0536744). The authors would also like to thank Dr. Leonid Zhigilei for his insights.

References

1. T.-D. Yuan, B.Z. Hong, H.-H. Chen, L.-K. Wang, Microelectron. Reliab. **42**, 101 (2002)
2. F. Ernst, Mater. Sci. Eng. **14**, 97 (1995)
3. P.L. Kapitza, Zh. eksp. teor. fiziki **11**, 1 (1941)
4. R.J. Stevens, A.N. Smith, P.M. Norris, J. Heat Transfer **127**, 315 (2005)
5. W.S. Capinski, H.J. Maris, T. Ruf, M. Cardona, K. Ploog, D.S. Katzer, Phys. Rev. B **59**, 8105 (1999)
6. K.E. Goodson, Y.S. Ju, Ann. Rev. Mater. Sci. **29**, 261 (1999)
7. C. Kittel, *Introduction to Solid State Physics*, 7th edn. (Wiley, New York, 1996)
8. E.T. Swartz, R.O. Pohl, Appl. Phys. Lett. **51**, 2200 (1987)
9. E.T. Swartz, R.O. Pohl, Rev. Mod. Phys. **61**, 605 (1989)
10. S.-H. Choi, S. Maruyama, Int. J. Therm. Sci. **44**, 547 (2005)
11. P. Reddy, K. Castelino, A. Majumdar, Appl. Phys. Lett. **87**, 211908 (2005)
12. M.S. Daw, M.I. Baskes, Phys. Rev. Lett. **50**, 1285 (1983)
13. S.M. Foiles, M.I. Baskes, M.S. Daw, Phys. Rev. B **33**, 7983 (1986)
14. M.S. Daw, M.I. Baskes, Phys. Rev. B **29**, 6443 (1984)
15. J.R. Lukes, D.Y. Li, X.-G. Liang, C.-L. Tien, Trans. ASME **122**, 536 (2000)
16. B.C. Gundrum, D.G. Cahill, R.S. Averback, Phys. Rev. B **72**, 1 (2005)